Thermo-Mechanical Fatigue Life Assessment of a Diesel Engine Piston

M. R. Ayatollahi*, F. Mohammadi and H. R. Chamani

[1] Professor, [2]MSc student, [3]PhD student, Faculty of Mechanical engineering, Iran University of Science and Technology. Tehran, Iran.

* m.ayat@iust.ac.ir

Abstract

In this study, a precise finite element analysis has been carried out on a diesel engine piston, in order to attain its high cycle fatigue (HCF) safety factor and low cycle fatigue (LCF) life. In order to calculate the HCF safety factor, a macro has been developed using ANSYS Parametric Design Language (APDL). The relative stress gradient parameter is used in order to perceive stress concentration and notch effect. In high cycle fatigue assessment, the effect of mean stress is considered using Haigh diagram. Different LCF life assessment methods have been used to investigate LCF life of piston and their results are compared to each other. The diesel engine piston is subjected to non-proportional multiaxial loading. The non-proportional loading leads to an additional cyclic hardening in the material. Critical plane LCF theories are appropriate for consideration of the additional cyclic hardening effect on the LCF life reduction of the piston.

Keywords: *Thermo-mechanical fatigue; Diesel engine piston; Critical plane; Low cycle fatigue; High cycle fatigue.*

1. INTRODUCTION

In recent years, increasing needs for higher power density, low emission and low fuel consumption impose many restrictions on the design process of diesel engine components. Therefore, the design and analysis methods of diesel engines have become substantially more complicated. Piston is one of the most challenging components in diesel engine which is subjected to high thermal and mechanical loads. Large temperature difference between piston crown and cooling galleries induces significant thermal load in piston. Besides, the firing pressure, piston acceleration and piston skirt side force can develop cyclic mechanical stresses which are superimposed on former thermal stresses. Therefore, thermo-mechanical fatigue is the main cause of failure in diesel engine piston.

The term "thermo-mechanical fatigue" (TMF) is used to describe fatigue in a component which is experiencing temperature and mechanical strain changes simultaneously [1].Under thermo-mechanical fatigue loading, total damage may occur due to fatigue, environmental degradation (oxidation) and creep mechanisms [2]. Thermo-mechanical fatigue life assessment methods can be classified as empirical methods, fracture mechanics theories, continuum mechanical models and models based on microstructure [3]. Empirical models correlate the number of cycles to failure to parameters of the hysteresis loop, e.g. stress, strain, plastic strain, etc.

Diesel engine piston is subjected to high temperature and multiaxial mechanical loading. Thermo-mechanical fatigue is the most important cause of failure in diesel engine piston, so its thermo-mechanical fatigue life estimation has to be done precisely. Piston's life assessment procedure must be comprehensive and suitable for complex geometry and non-proportional multiaxial loading conditions.

In this paper a precise procedure for the thermo-mechanical fatigue life assessment of a diesel engine piston is proposed. This procedure is outlined as follows:

- Determination of cyclic stress-strain distribution in piston under its loading conditions.
- Calculation of low cycle fatigue life of piston using appropriate theories.
- Calculation of high cycle fatigue safety factors.

A detailed thermo-mechanical stress analysis of piston has been performed. The thermal boundary conditions have been applied to finite element model of the piston. Temperature distribution of piston,

which has been obtained from the thermal analysis, has been applied as a volumetric load in structural analysis. In order to correctly model the material nonlinearity, a kinematic hardening model is used to simulate material behaviour. Different load steps of structural analysis consist of thermal loading, inertia loading, combustion pressure and piston skirt side force. The high cycle fatigue safety factors are calculated considering the mean stress effect by using Haigh diagram. Notch effect has been considered by using the relative stress gradient parameter. The critical plane low cycle fatigue (LCF) life assessment methods, appropriate for consideration of additional cycle hardening due to non-proportional loading, has been used to estimate LCF life of piston.

2. MATERIAL

Aluminum silicon alloys (predominantly eutectic) are widely employed to produce pistons due to their low density, high thermal conductivity, good castability and workability, good machinability and sound high temperature strength [4].

In this study the piston material is AlSi12CuMgNi cast alloy with eutectic microstructure. As all the engine components around the combustion chamber experience significantly high temperatures and temperature gradients, temperature dependent material properties have to be used. Some temperature dependent properties of piston material are shown in Table 1.

According to thermal analysis results maximum piston temperature reaches 374 °C, therefore cyclic behaviour of material is considered at 20, 150, 250 and 350 °C. The equation of uniaxial cyclic stress–strain curve is described as follows:

$$\varepsilon_a = \sigma_a / E + \left(\sigma_a / K'\right)^{\frac{1}{n'}} \tag{1}$$

where E is the Young's modulus, σ_a is the stress

Table 1. Temperature dependent properties of AlSi12CuMgNi [4].

Temp C	Conductivity W/mK	Tensile strength (GPa)	Elastic modulus (GPa)
20	155	0.2	80
150	156	0.18	77
250	159	0.09	72
350	164	0.035	69

Table 2. Values of   and   at different temperatures [5].

Temp C	cyclic strength coefficient K' (N/mm^2)	cyclic strain hardening exponent n'
20	402	0.11
150	370	0.11
250	241	0.11
350	104	0.11

Table 3. Fatigue limit of AlSi12CuMgNi at different temperatures [4].

Temp C	Fatigue limit N/mm^2
20	81
150	74
250	47
350	20

Table 4. Low cycle fatigue constants of AlSi12CuMgNi at different temperatures [5].

Temp C	Fatigue strength coefficient σ'_f	Fatigue strength exponent b	Fatigue ductility coefficient ε'_f	Fatigue ductility exponent c
20	211	-0.0539	0.013	-0.49
150	194	-0.0539	0.013	-0.49
250	118	-0.0539	0.0347	-0.49
350	44.7	-0.0539	0.13	-0.49

amplitude, ε_a is the strain amplitude, K' is the cyclic strength coefficient and n' is the cyclic strain hardening exponent. The values of K' and n' at different temperatures are listed in Table 2.

Fatigue limit and low cycle fatigue constants of AlSi12CuMgNi cast alloy at different temperatures are listed in Tables 3 and 4, respectively.

3. FINITE ELEMENT ANALYSIS

In order to perform thermo-mechanical fatigue analysis of the piston, one must have the piston cyclic stress-strain distribution in its loading conditions. Due to the complex geometry and loading of piston, analytical methods can't be applied to obtain its cyclic stress-strain distribution. Therefore, finite element (FE) analysis is applied to obtain the local stress–stain responses by simulating multiaxial loading conditions for piston.

The values of thermal stresses in the piston are

large enough and they may lead to low cycle fatigue failure. Besides, it may introduce high mean stresses and promote high cycle fatigue failure even in the regions with insignificant amplitude of cyclic mechanical loadings. Therefore, the temperature distribution and temperature gradient in the piston should be attained very accurately. The piston temperature is usually considered to be independent of the operating states and remains constant during a working cycle [6]. Since the time response of piston material to the variation of boundary conditions in a firing cycle is very slow, a steady state thermal analysis has been done considering the typical values of temperatures and heat transfer coefficients at piston boundary surfaces during one firing cycle. The boundary conditions considered for thermal analysis of the piston assembly can be summarized as:

- Temperature and heat transfer coefficient of hot combustion gases at piston crown.
- Temperature and heat transfer coefficient of cooling oil in piston cooling galleries.
- Heat transfer coefficient of piston and oil ring contact surfaces.
- Heat transfer coefficient of piston and compression rings contact surfaces.
- Heat transfer coefficient of piston and piston pin contact surfaces.
- Heat transfer coefficient at piston skirt.

Assuming a steady state thermal case, Fig. 1 shows some of the thermal boundary conditions of piston including the heat transfer coefficients and temperatures for the piston at different positions. These thermal boundary conditions were obtained from literature [7, 8] and modified based on brake mean effective pressure of current engine. Average temperature and heat transfer coefficient of hot combustion gases are obtained from one-dimensional thermodynamic analysis of engine cycle using Gt-Power software.

Fig. 2 illustrates the finite element model used for thermal analysis. This model includes piston and piston pin which is in contact with piston. The temperature distribution of the piston is shown in Fig. 3. Table 5 shows a comparison between the temperatures obtained from the present thermal analysis in some points of piston (shown in Fig. 3) and those given by the piston manufacturing company (MAHLE), which have been validated experimentally [9]. Good agreement can be seen between these two sets of results.

In order to attain the magnitude of stresses and stress gradients in the piston more precisely, the FE mesh has been refined in the contact and stress concentration regions. Figs. 4 and 5 show the FE mesh used for structural analysis of piston. In this analysis multilinear kinematic hardening model is used to deal with material nonlinearity. The following load cases are defined to simulate different stages of start-stop cycle:

1. Application of thermal loads (temperature).
2. Application of thermal loads, inertia loads

Steady-State Thermal
Time: 1. s
1/10/2011 2:28 PM

A Top-land: 300. °C, 200. W/m².°C
B Skirt: 115. °C, 500. W/m².°C
C 2nd-land: 115. °C, 120. W/m².°C
D 3rd-land: 115. °C, 120. W/m².°C
E Oil-ring: 115. °C, 200. W/m².°C
F 1st-ring-top: 115. °C, 700. W/m².°C
G 2nd-ring-top: 115. °C, 700. W/m².°C

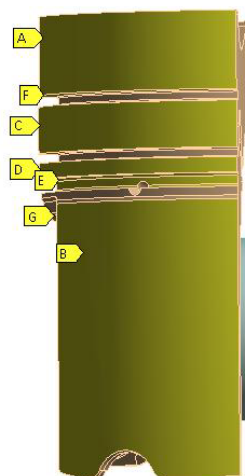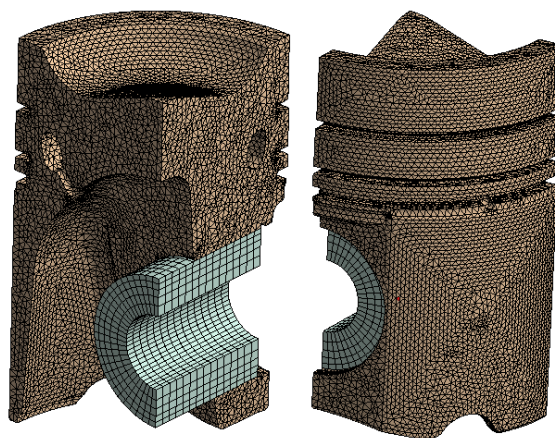**Fig. 1.** Thermal boundary conditions used in the

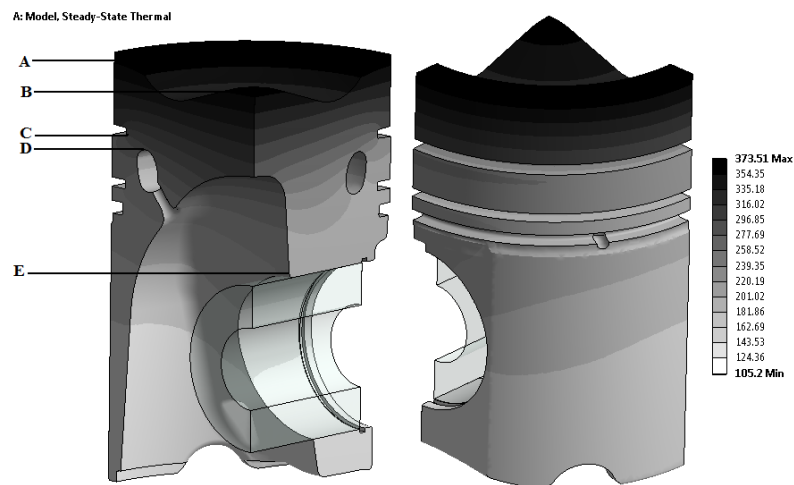**Fig. 2.** FE mesh used for thermal analysis of piston.

Fig. 3. Temperature distribution of the piston.

Table 5. Temperatures obtained from the thermal analysis in some points of piston (fig. 3) and Temperatures given by the piston manufacturing company (MAHLE).

	Temperatures gained by thermal analysis (˚C)	Temperatures given by the piston manufacturing company (˚C) [9]	Difference (%)
Point A	373	334	11
Point B	360	315	11
Point C	267	241	10
Point D	239	230	3
Point E	165	172	4

(piston acceleration), maximum pressure of combustion gases.

3. Application of thermal loads, inertia loads, pressure of combustion gases, maximum piston skirt side force.

4. Application of thermal loads and piston skirt side force.

5. Application of thermal loads and inertia loads.

6. Elimination of thermal loads and engine shutting down (ambient temperature).

Fig. 6 shows the structural boundary conditions applied to FE model of piston for structural analysis. Lateral planes are fixed in their normal directions, also the surface of pin (plane C in fig. 6) is fixed in the cylinder direction (z axis) in order to prevent rigid
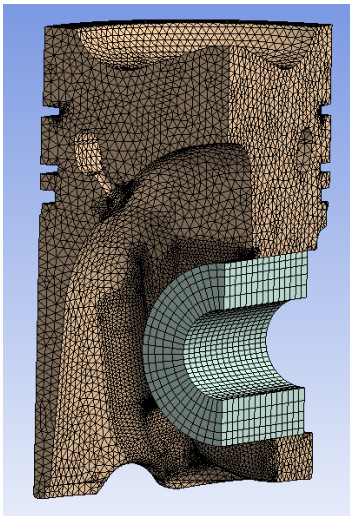

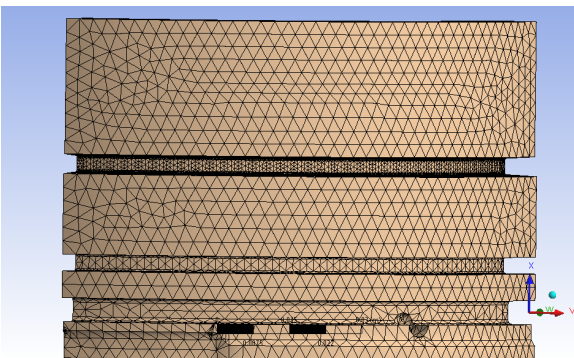**Fig. 4.** FE mesh used for structural analysis of piston.

Fig. 5. FE mesh in the region of piston rings used for structural analysis of piston.

B: Model, Static Structural

A — Displacement
B — Displacement 2
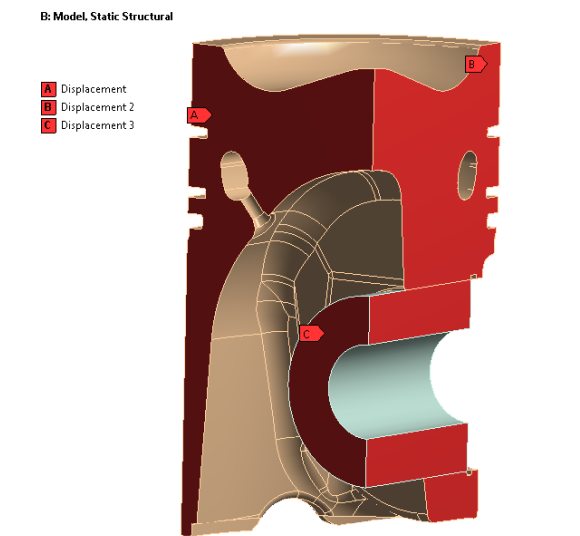C — Displacement 3

Fig. 6. Structural boundary conditions applied to FE model for structural analysis.

body motion. Further, the connection between the piston and piston pin was changed from the default "bonded" to "frictional" with a very low friction coefficient.

Fig. 7 shows the distribution of equivalent Von-

Mises stresses in the piston after application of thermal loads, inertia loads, pressure of combustion gases and maximum piston skirt side force. In the lower regions of piston skirt, close to oil inlet drillings, due to the reduction of piston wall thickness and stress concentration effect, the induced stresses are high. As can be seen in Fig. 7, the regions around the oil inlet hole and the contact regions of piston and piston pin are subjected to severe stresses. Table 6 gives the values of equivalent von-Mises stresses of critical points A and B, shown in Fig.7, at different steps of structural loading.

4. HIGH CYCLE FATIGUE LIFE ASSESSMENT

High cycle fatigue generally contains elastic cyclic behaviour, high frequency, low strain amplitude and large number of cycles to failure [10]. Constant life diagrams graphically represent the safe regime of constant amplitude loading for a given specified life and have been widely used for high cycle fatigue life estimation [11]. The Haigh diagram is a constant-life diagram that plots alternating stress versus mean stress and it is based upon Goodman equation [12]:

Table 6. Values of equivalent Von-Mises stresses of critical points A and B, shown in fig.7, at load steps 1 to 5.

Load step / point	Load step 1	Load step 2	Load step 3	Load step 4	Load step 5
A	1.3e7	6.3e6	9.4e7	4.8e7	6.1e6
B	3.4e7	1.9e7	5.1e7	3.8e7	4.2e7

1.6601e8 Max
1.5221e8
1.384e8
1.246e8
1.1079e8
9.6986e7
8.318e7
6.9375e7
5.5569e7
4.1764e7
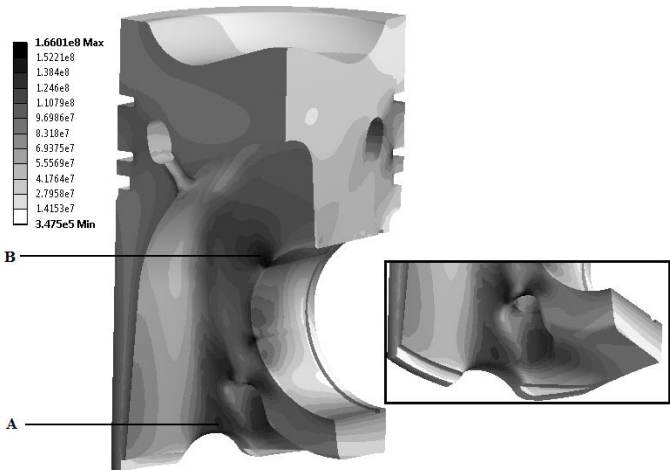2.7958e7
1.4153e7
3.475e5 Min

B

A

Fig. 7. Distribution of equivalent von Mises stresses in the piston due to thermal loads, inertia loads, pressure of combustion gases and maximum piston skirt side force.

$$\sigma_{alt} = \sigma_{R=-1}(1 - \frac{\sigma_{mean}}{\sigma_{UTS}}) \qquad (2)$$

where σ_{alt} is the alternating stress, σ_{mean} is the mean stress, $\sigma_{R=-1}$ is the stress amplitude at fully reversed loading, and σ_{UTS} is the ultimate tensile strength. The Haigh diagram can be used in order to consider the effect of mean stress in high cycle fatigue life estimation. Fig. 8 illustrates a scheme of the mean stress effect diagram or Haigh diagram.

By using Haigh diagram and calculating the equation of its lines and also having the magnitudes of the equivalent nominal stress amplitude and equivalent nominal mean stress, S_{qa} and S_{qm}, the high cycle fatigue safety factor of piston can be easily attained at each node of finite element model. Fig. 9 shows the Haigh diagram of piston material based on and FKM guideline [5].

The equivalent nominal stress amplitude, S_{qa}, has been computed according to the following relation:

$$S_{qa} = \frac{1}{\sqrt{2}} \sqrt{(\Delta S_{a1} - \Delta S_{a2})^2 + (\Delta S_{a2} - \Delta S_{a3})^2 + (\Delta S_{a1} - \Delta S_{a3})^2} \qquad (3)$$

where S_{a1}, S_{a2} and S_{a3} are principal alternating nominal stresses with $S_{a1} > S_{a2} > S_{a3}$.

The equivalent nominal mean stress, S_{qm}, has been computed as followes:

$$S_{qm} = \frac{1}{\sqrt{2}} \sqrt{(\Delta S_{m1} - \Delta S_{m2})^2 + (\Delta S_{m2} - \Delta S_{m3})^2 + (\Delta S_{m1} - \Delta S_{m3})^2} \qquad (4)$$

where S_{m1}, S_{m2} and S_{m3} are principal mean nominal stresses.

5. NOTCH EFFECT CONSIDERATION

When finite element method (FEM) is applied to assess HCF safety factor of notched components under dynamic loadings, it must be considered that FEM stress results give no indication of the type of the loading. When fatigue life estimation is going to be done with reference to tensile fatigue properties, inaccurate dimensioning may occur for the regions where bending/torsion stress is dominant. Moreover, real mechanical components generally contain many small fillets and blends, which can act as stress risers. Structural FE analysis gives notch a stress in these regions but this stress can't be used in the fatigue life calculations and must be modified somehow in order to get closer to the real amount experienced in the notch region.

Eichlseder [13] proposed a method for HCF safety factor assessment considering the load type and notch effect by using relative stress gradient parameter. The relation between fatigue limit and stress gradient can be determined as follows:
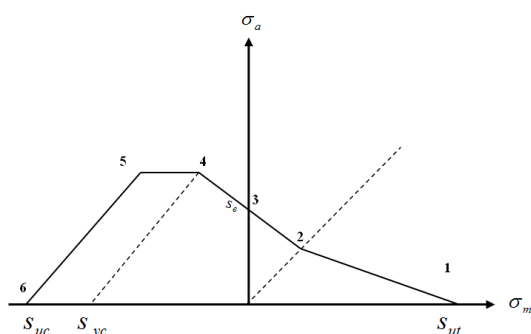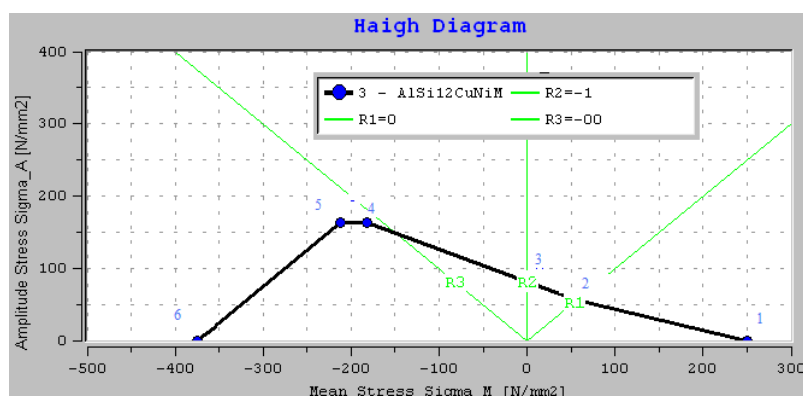

Fig. 8. Schematic of Haigh diagram.

Fig. 9. Haigh diagram of piston material [11].

$$\sigma_f = \sigma_{tf}\left[1+\left(\frac{\sigma_{bf}}{\sigma_{tf}}-1\right)\left(\frac{\chi}{2/b}\right)^{K_D}\right] \tag{5}$$

where σ_{tf} and σ_{bf} are fatigue limit in tension and bending respectively. b is the diameter of the specimen from which the bending fatigue limit is obtained. K_D is a material parameter in the range of 0.5 to 0.8 for engineering metals. For piston material K_D is considered as 0.6 approximately. Relative stress gradient χ is defined as:

$$\chi = \frac{1}{\sigma_{max}}\left(\frac{\partial\sigma}{\partial x}\right) \tag{6}$$

where σ_{max} is the notch root stress calculated by FEM. Therefore, in high cycle fatigue life prediction of components, it is needed to calculate the relative stress gradient at critical nodes of finite element model. Then, all of the material constants (fatigue limit, ultimate and yield stresses in tension and compression) must be corrected by using the stress gradient coefficient:

$$\lambda = \left[1+\left(\frac{\sigma_{bf}}{\sigma_{tf}}-1\right)\left(\frac{\chi}{2/b}\right)^{K_D}\right] \tag{7}$$

6. HCF LIFE ASSESSMENT IMPLEMENTATION AND RESULTS

In order to calculate the HCF safety factors, a macro has been developed using ANSYS Parametric Design Language (APDL). Haigh diagram is modified according to the magnitude of stress gradient, nodal temperature and modification factors at each node. The mean and alternating stresses resulted from cyclic loads are computed at each node. Then, HCF safety factor for each node is attained.

Fig. 10 shows the distribution of mean stresses in piston. Tensile and compressive mean stresses are observed in different regions of piston. Maximum tensile mean stresses due to inertia loads are observed in piston pin hole. Also in the regions near the oil and pressure rings, high tensile mean stresses are experienced. Fig. 11 shows the distribution of alternating stresses in piston. Maximum ranges of tensile alternating stresses are observed in the contact region of piston and piston pin and the regions around the oil inlet hole in piston skirt.
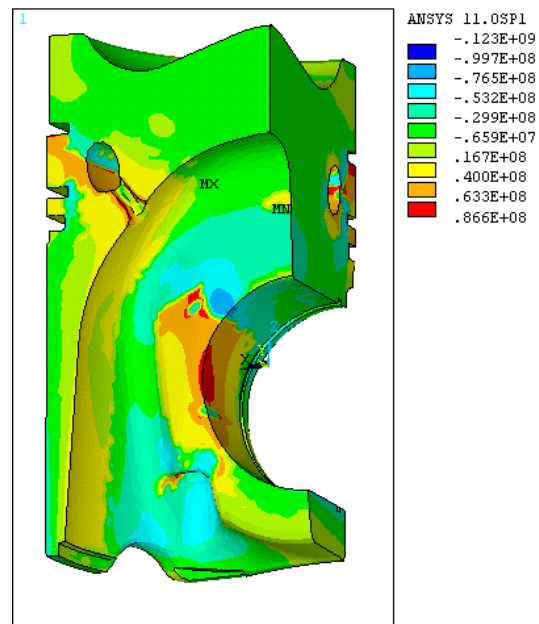

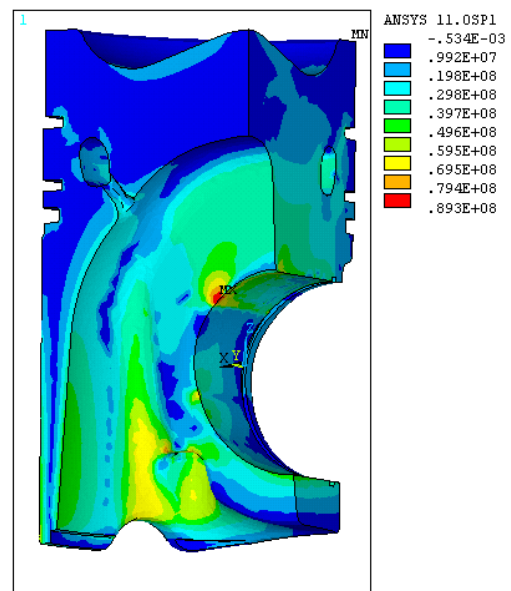**Fig. 10.** Distribution of mean stresses in piston.

Fig. 11. Distribution of alternating stresses in piston.

The contour of HCF safety factors in piston with and without considering the effect of stress gradient is shown in Fig.12 and Fig.13, respectively. The results show that after taking into account the beneficial effect of stress gradient, the minimum safety factor increased by 15% in the oil inlet hole and 50% in the pressure rings region.
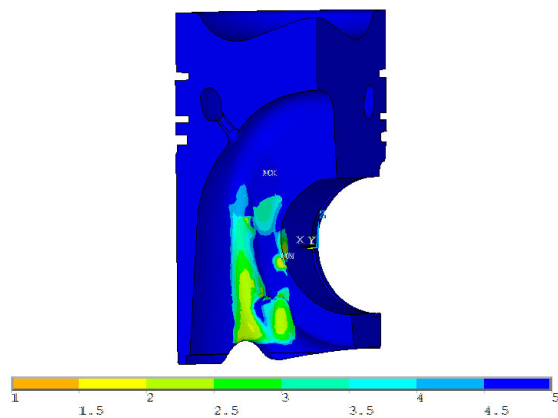
Fig. 12. Contour of HCF safety factor in piston after considering the effect of stress gradient.
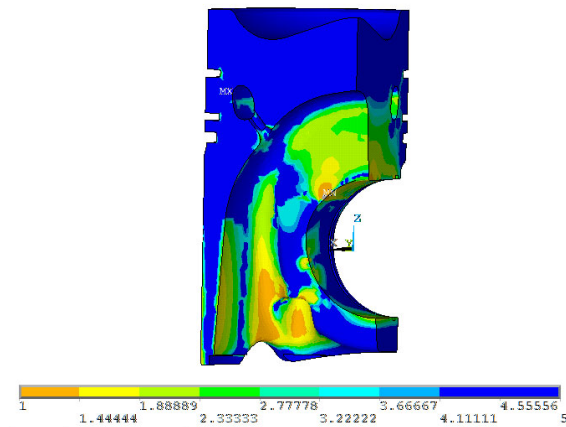

Fig. 13. Contour of HCF safety factor in piston before considering the effect of stress gradient.

7. LOW CYCLE FATIGUE LIFE ASSESSMENT

Up to now, various multiaxial fatigue damage models based on equivalent strain–stress, plastic work–energy and critical plane approaches have been proposed, but none of these models is universally accepted. Critical plane models have physical basis and consider the maximum principal strain/stress plane or the maximum shear strain/stress plane as the critical plane or the plane with maximum fatigue damage. These models are typically promising and applicable to both proportional and non-proportional loadings. Critical plane approaches can be classified into three categories as stress based models, strain based models and the models using both stress and strain terms [13]. Stress based models [15] are just

based on stress and are appropriate for high cycle fatigue regime that contains elastic deformation and small plastic strain. Strain based models [16] are suitable for loading condition with significant plasticity. Models which include both stress and strain terms [17, 18, 19] are suitable for materials that exhibit additional cyclic hardening due to the non-proportional loadings and normal stress term contained in these models can take into account the mean stress effects.

The Stress field in piston is multiaxial, so multiaxial fatigue models must be applied in the low cycle fatigue life assessment of piston. Also the fatigue loading of piston is complicated and nonproportional. Under nonproportional loading conditions, the additional hardening of material resulted from the rotation of the principal stress/strain axes is considered to result in the fatigue life reduction. In the present study, in order to account for the effect of additional cyclic hardening, critical plane approaches which include both stress and strain terms are used to estimate low cycle fatigue life of piston. Fatemi and Socie proposed the following model for low cycle fatigue life estimation [18]:

$$\frac{\Delta \gamma_{max}}{2}\left(1 + k \frac{\sigma_{n,\,max}}{\sigma_y}\right) = \left[\left(1 + v_e\right)\frac{\sigma'_f}{e}\left(2N_f\right)^b + \left(1 + v_p\right)\varepsilon'_f\left(2N_f\right)^c\right] \times \left(1 + k \frac{\sigma'_f}{2\sigma_y}\left(2N_f\right)^b\right) \qquad (8)$$

where N_f is low cycle fatigue life or number of cycles to failure, σ_y is the yield stress. v_e and v_p are elastic and plastic Poisson's ratios, b and c are fatigue strength exponent and fatigue ductility exponent, and ε'_f and σ'_f are fatigue ductility coefficient and fatigue strength coefficient, respectively. In this model the damage parameters governing fatigue life are the maximum shear strain range, $\Delta \gamma_{max}$, and maximum normal stress, $\sigma_{n,max}$, which is normal to the maximum shear strain range plane. Maximum normal stress is applied to reflect the effect of the additional cyclic hardening. k is an empirical constant and can be taken equal to 1.

Li et al. [19] proposed a new multiaxial fatigue damage parameter based on critical plane approach. The new damage parameter includes the strain parameter and the energy parameter where the normalized stress range is used:

$$\frac{\Delta\gamma_{\max}}{2}\left(1+\frac{\Delta\sigma_n}{2\sigma_y}\right)=\frac{\left(1+\left(1-\Delta\sigma_n/2\sigma_y\right)\nu_e\right)\sigma'_f}{E}\left(2N_f\right)^b+\frac{\sigma'^2_f}{\sigma_y E}\left(2N_f\right)^{2b}+ \qquad (9)$$

$$\cdot\frac{\left(1+\left(1-\Delta\sigma_n/2\sigma_y\right)0.5\right)\varepsilon'_f}{E}\left(2N_f\right)^c+\frac{\sigma'_f\varepsilon'_f}{\sigma_y}\left(2N_f\right)^{b+c}$$

This model uses maximum shear strain range, $\Delta\gamma_{\max}$, and range of normal stress, $\Delta\sigma_n$, in the damage parameter and is suitable for proportional and nonproportional loading conditions.

Recently, Li et al. [20] modified Shang–Wang fatigue damage parameter. The modified damage parameter combines maximum shear strain range with normal strain range on the critical plane, and a new stress-correlated factor, $\left(1+\frac{\Delta\sigma_n}{2\sigma_y}\right)$, is introduced to take account of the additional cyclic hardening:

$$\left(\frac{\Delta\gamma_{\max}^2}{3}+\left(1+\frac{\Delta\sigma_n}{2\sigma_y}\right)^2\Delta\sigma_n^2\right)^2=\frac{\left(1+\left(1-\Delta\sigma_n/2\sigma_y\right)\nu_e\right)\sigma'_f}{\sqrt{3}E}\left(2N_f\right)^b+ \qquad (10)$$

$$+\frac{\sigma'^2_f}{\sigma_y E}\left(2N_f\right)^{2b}+\frac{\left(1+\left(1+\Delta\sigma_n/2\sigma_y\right)0.5\right)\varepsilon'_f}{\sqrt{3}}\left(2N_f\right)^c+\frac{\sigma'_f\varepsilon'_f}{\sigma_y}\left(2N_f\right)^{b+c}$$

where $\Delta\gamma_{\max}$ is the maximum shear strain range. $\Delta\sigma_n$ is the range of normal stress. This model can be applied under both proportional and nonproportional loading conditions.

8. DETERMINATION OF CRITICAL PLANE

Most fatigue cracks initiate in the maximum shear direction because the slip systems which align in these directions experience the largest amount of deformation. But cracks also initiate at a slower rate in the directions with less degrees of shear [21]. Therefore, it can be assumed that maximum fatigue damage occurs at the plane of maximum shear strain amplitude. This plane is called the critical plane. In order to determine the maximum shear strain range plane or critical plane, one must take the following steps [22]:

1.   Determine the stress and strain tensors at all nodes of FE model by carrying out an elasto-plastic finite element analysis for the component.
2.   Consider a candidate plane at the target node (the node which its low cycle fatigue life is going to be calculated) defined by angles θ and φ (Fig. 14).
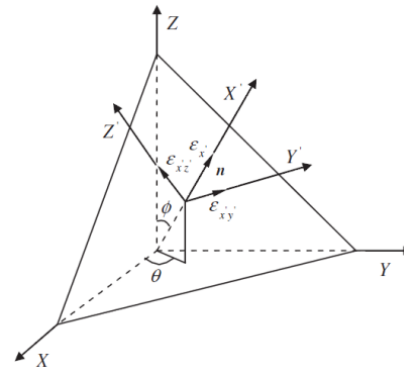3.   Calculate the stress and strain tensors on the

Fig. 14. The strains acting on the candidate plane at the target node [14].

candidate plane.
4.   Calculate the shear strain range acting on the candidate plane.
5.   Solve for Steps 3 and 4 for all planes in order to find the maximum shear strain range planes and their locations.
6.   Calculate the normal strain ranges acting on the maximum shear strain range planes.
7.   Compare the values of the normal strain range acting on the planes of maximum shear strain to determine the location (θ_{cr},ϕ_{cr}) of critical plane.

9. LCF LIFE ASSESSMENT IMPLEMENTATION AND RESULTS

In order to calculate LCF life of piston, a macro has been written using ANSYS Parametric Design Language (APDL). By using the stress-strain cycle at each node and according to critical plane approach, LCF life of piston has been calculated at each node. The algorithm of the developed macro is outlined as follows:

1.   Reading the data and temperature dependent material properties at each note.
2.   Determination of loading cycles.
3.   Selection of elements and nodes at which the low cycle fatigue life calculations is going to be done (the piston surface nodes must be selected).
4.   Reading the information of selected nodes such as node number, node coordinate and etc.
5.   Reading the stress analysis results at selected nodes (according to the applied LCF life model the needed information such as stresses, strains must be read and saved in array parameters).
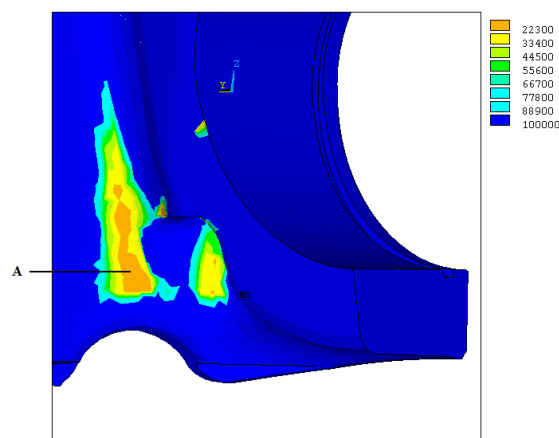
Fig. 15. Contour of LCF life of piston calculated by Li model (Eq. 10).

6. Finding critical plane at each node.
7. Calculation of damage parameter at critical plane.
8. Calculation of LCF life according to the applied model.

The LCF life contour of piston using Li (Eqs. 9 and 10) model is shown in Fig. 15. Number of LCF life cycles calculated by Fatemi - Socie (Eq. 8) and Li (Eqs. 9 and 10) models at critical point A (fig. 15), are 27000, 22000 and 21000 cycles, respectively. The estimated LCF lives resulted from these models are very close to each other. The regions around the oil inlet hole in piston skirt are the critical regions from the LCF life point of view.

10. CONCLUSIONS

In this study, a detailed thermo-mechanical stress analysis has been conducted on a diesel engine piston. Temperature distribution has been obtained from thermal analysis. In order to attain HCF safety factor, a macro has been developed using ANSYS Parametric Design Language (APDL). Then a Haigh diagram is established for each node based on the calculated stress gradient and nodal temperature. In order to account for the effect of additional cyclic hardening, critical plane approaches which include both stress and strain terms are used to estimate low cycle fatigue life of piston. The plane experiencing the maximum shear strain amplitude is considered as the critical plane.

The results showed that the regions around piston oil inlet hole and the piston and piston pin contact region are the most critical regions, mainly due to high mean and alternating stresses caused by cyclic loads. After considering the stress gradient effects, the HCF safety factor improved by 15% in the oil inlet hole and 50% in the pressure rings region. The regions around the oil inlet hole in piston skirt are the critical regions from the LCF life point of view.

REFERENCES

[1]   Asm Metals Handbook Volume 19 – Fatigue and Fracture.

[2]   Gocmez, T., Awarke, A., Pischinger, S., 2010, "A New Low Cycle Fatigue Criterion For Isothermal And Out-Of-Phase Thermomechanical Loading", Int. J. Fatigue, 32, 769-779.

[3]   Minichmayr, R., Riedler, M., Winter, G., Leitner, H., Eichlseder, W., 2008, "Thermo-Mechanical Fatigue Life Assessment Of Aluminium Components Using The Damage Rate Model Of Sehitoglu", Int. J. Fatigue, 30, 298–304.

[4]   K. Mollenhauer, H. Tschoeke, Handbook of Diesel Engines, Springer Heidelberg Dordrecht London New York.

[5]   FKM guideline "Numerical Strength Analyses for Machine Components in Steel, Cast Iron and Aluminum Materials", 4th Edition, 2002.

[6]   P. Gudimetal, C.V. Gopinath, 2009, "Finite Element Analysis of Reverse Engineered Internal Combustion Engine Piston ", AIJSTPME, 2(4), 85-92.

[7]   J. Pan, R. Nigro, E. Matsuo, 2005, "3-D Modeling Of Heat Transfer In Diesel Engine Piston Cooling Galleries", SAE International.

[8]   V.P. Singth, P.C. Upadhyay, N.K. Samria, 1986, "Some Heat Transfer Studies On A Diesel Engine Piston", lnt. J. Heat Mass Transfer, 5, 812-814.

[9]   MAHLE technical report, Projekt 6500-01595-01, Nr. PDE08-0070-65.

[10] Nicholas, T., 2006, "High Cycle Fatigue, A Mechanics of Materials Perspective", 1st edition, Elsevier.

[11] Sendeckyj G.P., 2001, "Constant life diagrams — a historical review", International Journal of Fatigue, 23, 347–353.

[12] Lanning, D. B., Nicholas, T., 2007, "Constant-life diagram modified for notch plasticity". Int. J. of Fatigue, 29, 2163–2169.

[13] Eichlseder, w., 2002, "Fatigue analysis by local stress concept based on finite element results". J Computers and Structures, 80, 2109–2113.

[14] Li, J., Zhang, Ping, Z., Sun, Q., Li, Ch. W., 2011, "Multiaxial fatigue life prediction for various metallic materials based on the critical plane approach", International Journal of Fatigue, 33, 90–101.

[15] Susmel, L., 2011, "On The Overall Accuracy Of The Modified Wöhler Curve Method In Estimating High-Cycle Multi axial Fatigue Strength", Frattura Ed Integrità Strutturale, 16, 5-17;

[16] Borodii, M.V., Adamchuk, M.P., 2009, "Life assessment for metallic materials with the use of the strain criterion for low cycle fatigue", International Journal of Fatigue, 31, 1579–1587.

[17] Varvani-Farahani, A., Kodric, T., Ghahramani, A., 2005, "A method of fatigue life prediction in notched and un-notched components", Journal of Materials Processing Technology, 169, 94–102.

[18] Fatemi, A., Socie, D. F., 1988, "A critical plane to multiaxial fatigue damage including out-of-phase loading", Fatigue Fract Eng Mater Struct, 11, 149-165.

[19]. Li, J., Zhang, Z. P., Sun, Q., Li C. W., Qiao, Y. J., 2009, "A new multiaxial fatigue damage model for various metallic materials under the combination of tension and torsion loadings". I. J. Fatigue, 31, 776–781.

[20] Li, J., Zhang, Z. P., Sun, Q., Li C. W., Qiao, Y. J., 2010, "A modification of Shang–Wang fatigue damage parameter to account for additional hardening". Int. J. Fatigue, 32, 1675–1682.

[21] Susmel, L., Atzori, B., Meneghetti, G., Taylor, D., 2011, "Notch And Mean Stress Effect In Fatigue As Phenomena Of Elasto-Plastic Inherent Multiaxiality". Engineering Fracture Mechanics, Article in Press.

Nomenclature

b	Fatigue strength exponent
c	Fatigue ductility exponent
E	Young's modulus
K_t	Stress concentration factor
N_f	Number of cycles to failure
ε'_f	Fatigue ductility coefficient
ε_a	Maximum principal strain amplitude
σ_i	principal stress (i=1,2,3)
σ_{fb}	Bending fatigue limit
σ_{ft}	Tension fatigue limit
σ'_f	Fatigue strength coefficient
σ_{max}	Maximum normal stress
τ_{ft}	Shear fatigue limit
χ	Relative stress gradient
ν_e	Elastic Poisson's ratio
ν_p	Plastic Poisson's ratio